Iğdır Üniversitesi Fen Bilimleri Enstitüsü Dergisi, 13(3), 1804-1813, 2023
Journal of the Institute of Science and Technology, 13(3), 1804-1813, 2023

ISSN: 2146-0574, eISSN: 2536-4618

Kimya / *Chemistry* **DOI: 10.21597/jist.1264079**

Araştırma Makalesi / *Research Article*

Geliş tarihi / *Received*: 12.03.2023 **Kabul tarihi / *Accepted*: 27.05.2023**

Atıf İçin: Ateş, M. N. (2023). Elektro Kaplama Yöntemi ile Elde Edilen Kalay Anodunun Lityum İyon Pillerde Performansının İncelenmesi. *Iğdır Üniversitesi Fen Bilimleri Enstitüsü Dergisi*, 13(3), 1804-1813.

To Cite: Ateş, M. N. (2023). Understanding the Effect of Deposition Potential on the Electrodeposited Tin Anodes for Lithium-Ion Batteriesı. *Journal of the Institute of Science and Technology*, 13(3), 1804-1813.

Elektro Kaplama Yöntemi ile Elde Edilen Kalay Anodunun Lityum İyon Pillerde Performansının İncelenmesi

Mehmet Nurullah ATEŞ

Öne Çıkanlar:
- Kaplama Potansiyelinin Etkisi
- Lityum İyon Anot Performans İncelenmesi
- Parçacık Boyut analizi

Anahtar Kelimeler:
- Elektro kaplama
- Kalay anot
- Lityum İyon
- Anot Aktif Malzeme
- Elektrokimya

ÖZET:

Kalay (Sn), Li-ion piller için gelişmekte olan alternatif bir anot adayıdır. Bolca bulunması ve düşük maliyeti nedeniyle araştırmacılar, Li-ion piller (LIP) için yeni nesil bir anot alternatifi olarak Sn anot üzerinde çalışmaktadırlar. Bu çalışmada sulu ortamdan elde edilen elektrolizle kaplanmış Sn anodunu inceledik. Bakır akım toplayıcı üzerinde saf kalay anot sentezlemek için elektro kaplama yöntemini kullandık. Kalay tuzu, yüzey aktivatörü, yapıştırıcı ajan, tamponlama ve kompleks yapıcıdan oluşan sulu ortam, herhangi bir bağlayıcı ve iletken ajan kullanılmadan saf kalay elde etmek için kullanılmıştır. Biriktirme potansiyelleri ve bunların partikül morfolojisi ve kristal yapısı üzerindeki etkileri araştırıldı. Elektrokimyasal performansı arttırmak için kalay anodu iletken polimer kaplama ile kapladık ve ısıl işlemin polimer kaplı kalay anotlar üzerindeki etkisini inceledik. Elektro kaplama ile Sn elektrodun elektrokimyasal performansı ve fiziko kimyasal özellikleri, Taramalı elektron mikroskobu, X-ışını Kırınımı ve elektrokimyasal tekniklerle karakterize edildi. Kaplama potansiyelinin voltajı arttırıldıkça kalay parçacıklarının daha da büyüdüğü gözlemlenmiştir. X-ışını kırınımı sonuçlarında farklılık gözükmemiştir. -0.8V ve -0.9V kaplama voltaj değerleri ideal elektrokimyasal sonuçları vermiştir. Polimer kaplamanın ilk kapasite değerine olumlu etkisi olsa da döngü ömründe yeteri iyileştirme oluşturmadığı gözlemlenmiştir.

Understanding the Effect of Deposition Potential on the Electrodeposited Tin Anodes for Lithium-Ion Batteries

Highlights:
- Effect of Deposition Potential of Tin
- Particle Growth Mechanism
- Lithium Ion cell performance

Keywords:
- Deposition of Tin
- Lithium Ion
- Anot Active Material
- Electrochemistry
- Tin Anode

ABSTRACT:

Tin (Sn) is an emerging anode candidate for Li-ion batteries. Due to its high availability and low cost, researchers are studying Sn anode as a next-generation anode alternative for Li-ion batteries (LIB). In this study, we have investigated the electroplated Sn anode obtained from the aqueous media. We have utilized the electrodeposition method for synthesizing pure tin anode on the copper current collector. Aqueous media comprised of tin salt, surface activator, adhesive agent, buffering, and the complexing agent was utilized for obtaining pure tin without using any binder and a conductive agent. Deposition potentials and their effect on the particle morphology and crystal structure were investigated. To enhance the electrochemical performance, we coated the tin anode with the conducting polymer coating and further analyzed the effect of the heat treatment on the polymer-coated tin anodes. The electrochemical performance and physicochemical properties of the electrodeposited Sn electrode were characterized by, Scanning electron microscopy, X-ray Diffraction, and electrochemical techniques. As the voltage of the coating potential increases, it has been observed that the tin particles further enlarge. No difference is observed in X-ray diffraction results for the tin electrodes obtained at different voltages. Coating voltage values of -0.8V and -0.9V have provided ideal electrochemical results. Although polymer coating has a positive effect on the initial capacity value, it has been observed that it does not have sufficient improvement in cycle life.

Mehmet Nurullah Ateş (**Orcid ID:** 0000-0002-3557-6769), Department of Chemistry, Boğazici University, Bebek, Istanbul, Türkiye

***Corresponding Author:** Mehmet Nurullah Ateş, e-mail: mehmet.ates@boun.edu.tr

A part of the submitted article was presented as an oral presentation at the 2nd World Energy Storage Congress held in Istanbul on 18-21 December 2022.

INTRODUCTION

Graphite is the most used anode active materials in lithium ion batteries commercially used nowadays. However, the capacity of the Graphite is only limited to around 372mAh/g. In order to enhance energy density of current state of the art lithium ion batteries, researchers are pursuing next generation anode active materials. Among these materials Lithium, Silicon and Tin are promising anode materials due to higher capacities. Lithium metal anode based batteries require solid state battery technology to be matured. Silicon on the other hand posses' high capacities of 4212 mAh/g whereas it experiences dramatic volume expansion and contraction during cycling. Si also is not conductive creating rate problems for lithium ion batteries. Tin(Sn) is a promising anode candidate for Li-ion battery with a theoretical capacity of 993 mAh/g. Low cost, high abundance, good electrical conductivity and low toxicity triggered the interest for Sn based anode active materials for Lithium ion batteries (LIBs)(Han, Liu, & Ivey, 2009). Although Sn based anodes similar to Si anodes experience volume expansions, it provides high electrical conductivity allowing fast charge capabilities. The precursors used during the synthesis of Sn active materials are sustainable and cheap unlike Si based anodes where Silane based precursors are utilized such as $SiCl_4$ or $SiHCl_3$. Though Sn has such advantages still it suffers from volume expansion which causes drastic capacity fade during cycling. One way to mitigate the capacity fade is through encapsulation of Sn particles with carbon. Zhen Kong and his colleagues showed that if the Sn nanoparticles are encapsulated with graphene, both the rate and cycle life properties of Sn anode improved significantly (Kong et al., 2022). Scrosati and his friends also carried out similar studies where Sn-C composite anodes were synthesized to overcome the barriers of traditional pure Sn anode has. The synthesis method was based on carbonization of Resorcinol-Formaldehyde gel where the Sn metal particles were embedded. The anode produced with this way revealed an outstanding cycle life capabilities extending hundreds of cycles without any capacity fade (Derrien, Hassoun, Panero, & Scrosati, 2007). Baolian Yi and his team reported that the composite of Sn with carbon nano tubes (CNT) can improve the cycle life of Sn based anode composites. They utilized chemical reduction method to obtain Sn/CNT composite which showed 70% capacity retention after 100 cycles (Wu, Wang, Chen, Wang, & Yi, 2013). In this study we have focused on how particle size of tin crystals can be controlled via electroplating parameters.

Electrochemical deposition is a powerful technique which is used to deposit pure metal as well as alloys(Ates & Busbee, 2017; Sohel et al., 2022; Yue et al., 2021; Zheng et al., 2020). It has many advantages such as obtaining battery grade purity materials at low temperature. Several studies have been performed by researchers on the electrodeposition of tin from acidic and alkaline media(Ashworth et al., 2015; Dirican et al., 2014; He, Liu, & Ivey, 2008; Huang, Chen, Fu, Zhang, & Zhang, 2013; Lee, Kim, Chang, Tae Kim, & Park, 2004; Tirado, 2003; Torrent-Burgués, Guaus, & Sanz, 2002; Walsh & Low, 2016; Zhang & Abys, 1999). These studies discussed in great detail about tin deposition mechanism and its properties without performing electrochemical performance analysis. Binary-phase of Li-Sn diagram suggests that when reacted with lithium, Sn forms seven different phases such as LiSn, Li_2Sn_5, Li_5Sn_2, Li_7Sn_2, Li_7Sn_3, $Li_{22}Sn_5$, and $Li_{13}Sn_5$ (Tirado, 2003) allowing high Li storage capacity which makes Tin a promising next generation anode for Li-ion batteries.

Yun Zhang et al. (Zhang & Abys, 1999) have proposed a novel chemistry bath for tin deposition which produces stain bright tin with large grain size and almost possess 100% plating efficiency. They have deposited tin on Cu substrate from an acidic bath and reported some of its mechanical properties without mentioning the electrochemical behavior in batteries. Anqiang He et al. (He et al., 2008) reported tin deposition from a slightly acidic aqueous bath where tin (II) chloride was used as

precursor. They reported constant current tin deposition and its characteristics through SEM/EDS and XRD analysis but no electrochemical tests were performed. S.S. Abd El Rehim et al.(Abd El Rehim, Sayyah, & El Deeb, 2000) have carried out a similar study on tin deposition form aqueous bath of stannous sulfate, sodium gluconate and potassium sulfate. They have deposited tin on steel substrate and carried out detailed deposition parameter and their effect on polarization, structure and morphology of deposited tin. Xianqiu Huang et al. (Huang et al., 2013) have reported tin deposition investigated with the help of electrochemical impedance technique. They have reported detailed deposition parameter studies and proposed that charge transfer resistance of tin deposition exponentially decreases with the biasing potential. M.A. Ashworth et. al.(Ashworth et al., 2015) have reported the effect of tin deposition parameter and substrate on the formation of tin whisker and proposed how this whisker growth can be minimized by controlling the electrochemical deposition parameters.

Koichi Ui et. al. (Ui, Kikuchi, Kadoma, Kumagai, & Ito, 2009) have proposed pulse current electrodeposition of pure tin and presented coin cell data comparison between constant current and pulse current tin plating. Constant current suffers sharp capacity degradation after 10 cycles where pulse current maintains decent capacity even after 20 cycles. Ou Mao et al (Mao, Dunlap, & Dahn, 1999) have proposed mechanical alloying anode of Sn-Fe(-C) composite where sharp decrement of capacity has been observed as well after 10 cycles.

As it is shown in the literature crystallinity and particle size can greatly influence the electrochemical performance of tin anode materials (Wang, Luo, Li, & Zhi, 2012). In this study, we have revealed that the deposition potential greatly influences the particle size and crystal shape albeit no XRD difference was observed. At extreme deposition voltages (both at the lowest and highest), the specific capacity of tin anode was worse than the other two sets revealing the importance of particle size.

MATERIALS AND METHODS

Chemicals

Stannous Chloride, dihydrate ($SnCl_2.2H_2O$), Potassium Pyrophosphate ($K_4P_2O_7$), Glycine ($C_2H_5NO_2$) and Polyvinylpyrrolidone (PVP) and Polyvinylidene Chloride (PVDC) were bought from Sigma Aldrich and used as received. Deionized (DI) water, Tin metal flakes (Sn) and Pt wire were also used as solvent, counter electrode and reference electrode, respectively. Tin metal counter electrode were prepared by melting the spherical tin powders and forming the foil by cooling the molten Sn.

Deposition Medium

The tin deposition bath was prepared by dissolving the precursors in aqueous media (distilled water) sequential order. At first, Potassium Pyrophosphate was dissolved in DI water with the help of magnetic stirrer with a rotation speed of 200rpm. This is followed by the addition of Glycine which is followed by dissolving Stannous Chloride dihydrate.

Morphological and Structural Characterization

X-ray diffraction (XRD, Rigaku Miniflex) was used to unravel the crystal structure of tin with Cu Kα radiation (40 kV, 15 mA). Electrodes were cut from the Copper foil and directly stuck on the aluminum sample holders for the XRD measurements. Scanning electron microscopy (SEM) were performed using a JEOL JSM 6510LV instrument to analyze surface morphology. For the cross-section SEM images, the electrodes were broken from the center of the Cu foil. All the characterization samples were prepared under the same condition on commercial Cu foil.

Coin Cell Preparation and Electrochemical Characterization

CR2032 type half-cell was prepared in an Ar-filled glove box (Vigor) using 1M $LiPF_6$ (lithium hexafluorophosphate) in ethylene carbonate (EC): dimethyl carbonate (DMC): diethyl carbonate (DEC) (1:1:1) as the electrolyte and Li metal foil as cathode. 14mm diameter circular electrodes were cut from the one sided tin deposited Cu foil and used as working electrode in half cells. The amount of Tin on Cu foil was around $2mg/cm^2$ and weighing of tin was simply calculated with the balance. Large Cu foil 4cm*9cm was weighed before deposition and tin deposition was performed on this foil. Later tin coated Cu foil was weighed and the difference was calculated for tin. The deposition uniformity was controlled by thickness and found to be uniform. Coin cells were tested at room temperature using Neware CT-4008T battery cycler. To produce single side tin coated Cu foil, before the deposition, PVDC was casted on Cu foil and dried where the non-conductive PVDC adhered to the foil and allowed us to plate Sn only the surface where PVDC is not coated. Single side tin coating was a necessary step to construct coin cells. All the cells were kept under rest for 4 hours before executing the cycle life test to clinch complete penetration of electrolyte. Every cell was lithiated (charged) to 0.01 V and delithiated (discharged) to 1.50 V with constant current constant voltage (CC) mode.

RESULTS AND DISCUSSION

In order to understand the deposition mechanism, cyclic voltammetry (CV) has been utilized as the most effective method. This study was also started with the CV experiment of each solution preparation step. The CV scanning was carried out at the rate of 500μV/s between OCP to -1.0 V using AUTOLAB PGSTAT 302 N (Metrohm, Netherlands). Note that in all the cases, the Working Electrode (WE) was Platinum foil, Counter Electrode (CE) was Pure Tin plate and Quasi Reference Electrode (QRE) was Platinum wire. First CV test was executed after dissolving Potassium Pyrophosphate in DI water and the result is shown with blue colored line in Figure 1A. No current flow was observed on Pt foil WE indicating no reaction or reduction started which is expected as Potassium pyrophosphate is used as surface treatment agent. After dissolving Glycine in the same solution, CV scanning was preformed again on the refreshed electrodes and the result is depicted with green line in Figure 1A. Glycine is used as buffering agent. This time very small amount of current flow was observed on WE started around at 0.85V. This tiny current flow might indicate that minor electrochemical reaction occurred. The unwanted reduction can be ignored or avoided if the final solute addition can shift the desired tin reduction potential towards the positive direction. Following this experiment, the Stannous Chloride, dihydrate was added on the replenished electrodes and CV test was executed. This CV result is shown with red colored line in Figure 1A. At this time, the electrochemical reduction reaction started at -0.7V with significant amount of current flow on Pt foil surface. This reduction is directly related to the Sn reduction and followed by deposition on WE. The reduction current reached to its peak at -0.8V which was further reduced during continuous forward scan to -1.0V. Further forward scan was avoided as the water electrolysis and hydrogen (H_2) gas evolution was observed in a separate experiment. Finally, the same CV experiment was carried out on Cu foil keeping all the conditions and parameter the same and the result is shown with yellow color in Figure 1A. In this CV curve, significant reduction current started to flow at -0.7V as before (red curve) which reached to maximum at -0.8V suggesting peak reduction occurred at that potential. Significant amount of current flown all the way to -1.0V identical to the reaction where Pt was used as working electrode. Therefore, for the cathodic deposition of tin (Sn) on Cu foil substrate, -0.7, -0.8, -0.9 and -1.0V was chosen for constant voltage deposition in order to compare their morphology and structure. Figure 1B shows the currents generated during the tin deposition at different potentials. As expected

the lower the reduction potential is applied during Sn plating, the higher the current is generated. This in turn leads slightly higher loading for Sn films obtained at lower potentials (-1V) at the same deposition duration. This is expected since the more negative potential is applied to the deposition medium the more Sn is reduced to balance the neutrality. Usually deposited materials can lead resistance during deposition however Sn has metallic conductivity which does not yield significant resistance.

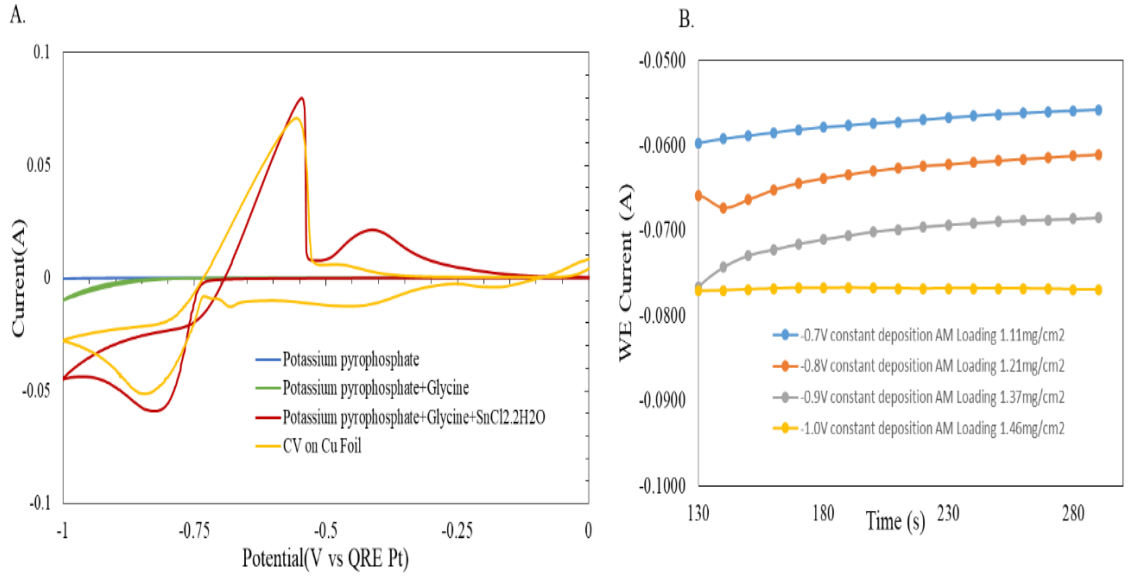

Figure 1. A-) Cyclic Voltammetry of tin deposition medium at each step of chemical addition to the deposition bath. B-) Current generated during the electrodeposition of Sn at different potentials versus time

Constant voltage deposition was carried out for the same time at those four different potentials and the structure, morphology and elemental analysis was performed through SEM/EDS. The morphology and elemental composition was examined through SEM/EDS analysis which is shown in Figure 2A-D. As four different potentials was chosen to deposit tin and compare, from their SEM images it is clear that with the increment of deposition potential, deposited tin morphology is changing significantly. At -0.7V shown in Figure 2A, which can be considered as under potential deposition, tin was not able to cover the whole Cu surface during constant voltage deposition. As a result, the amount of deposited tin was less compared to the deposition took place at lower potentials. Deposition at -0.8V was different as visible from Figure 2B. As the deposition potential increased, the grain boundary was more visible and the particles started to segregate from each other depicted in Figure 2B. This particle size increase gets much clearer when the deposition was further decreased to -0.9V and -1V which are shown in Figure 2C and 2D. The cross sectional images presented in Figure 2A-D are suggesting the thickness of the deposited tin increased with the increment in deposition potential at the same deposition time. The highest dendrite formation was visible for -1.0V deposition. As the tin dendrite is not expected, it also affected the anode quality found during cell cycle life test. EDS data, not shown in here, demonstrated that elemental composition was very similar to each other with no other elements present on the electrode. The exception for the additional element was Cu as the substrate of tin deposition was performed on Cu foil.

Electrodeposited tin crystal structure was studied through XRD analysis and the data is presented in Figure 3. Representative of the XRD pattern is depicted in Figure 3 along with Cu foil as reference. In our study all of the samples deposited at different potentials revealed the similar XRD patterns. Note that the strong Cu peak around 42, 50 and 74 2θ degrees indicates that the X-ray might have penetrated through the uncovered area and revealed the Cu presence in the pattern.

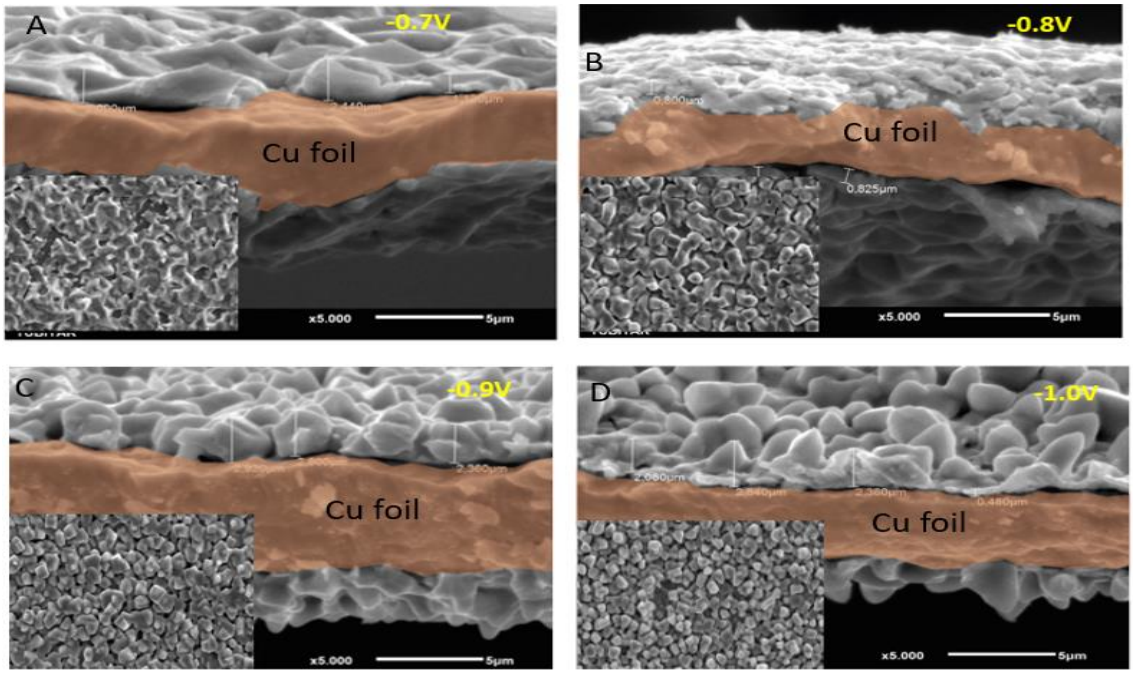

Figure 2. SEM images for electrodeposited tin on Cu foil at different constant potentials. Inset images show the surface feature of the tin deposited Cu foil at different potentials. Sn deposition on Cu foil at constant voltages A-) at -0.7V B-) at -0.8V C-) at -0.9V and D-) at -1V

This is expected since the deposition thickness was few microns allowing X-ray penetration through the Sn film. From XRD data of our prepared sample and the reference data for Cu, we can conclude that we electrodeposited beta phase Tetragonal tin crystal phase (Cross-Ref PDF # 00-004-0673). The finding bodes well with the reported literature on metallic tin (Ui et al. 2009). From the XRD it is hard to decide which voltage would be best for deposition as almost all the constant voltage depositions have the same crystallinity and similar peaks. As a result, to find the best quality tin for Li-ion battery anode, coin cells were prepared from all the four samples and the results were compared.

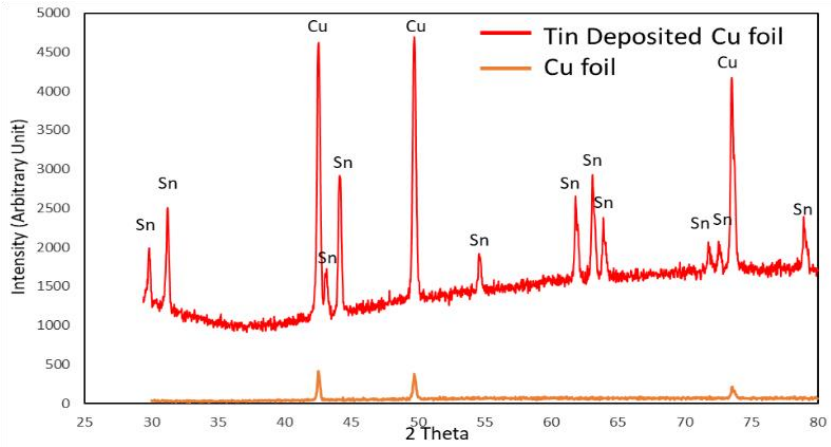

Figure 3. XRD data for the electrodeposited tin sample on Cu foil substrate

In order to unravel the performance of tin deposited electrode as anode, we have prepared and analyzed four different electrodes in lithium-ion cells. Sn-0.7, Sn-0.8, Sn-0.9 and Sn-1.0 nomenclature have been used for cells made of -0.7, -0.8, -0.9 and -1.0V constant voltage deposited tin electrodes, respectively. Figure 4A shows corresponding lithiation capacity. From this figure it is clear that the best electrochemical performances were obtained at -0.8V and -0.9V while the two extreme cases (the lowest deposition and highest deposition potential) revealed poorer performances. The low initial

capacity for the highest deposition (-1V) could be due to large grain size of tin, shown in Figure 2D, which causes kinetic hindering for lithium ions to be alloyed. However, during cycling the capacity gradually increase most likely due to cracking which allows new lithium alloying reaction mechanisms. For the lowest electrodeposited sample, i.e. -0.7V, the tin electrode also revealed lower capacity due to most likely not very well formed grains. The tin grains formed at -0.7V shows a sticky behavior unlike to other three samples as shown in Figure 2A. The cycle life performance obtained at 0.1C rate is depicted here. From the result it is clear that the capacity of all four types of electrodes started fading after 10 cycles and became significantly lower after 20 cycles. For Sn-0.7V and Sn-1.0V cell, the first charging (Lithiation) capacity was 315 and 255 mAh/g as depicted in Figure 4B, respectively. Those capacities start increasing afterwards and reached to maximum at 5th and 7th cycles, respectively. This increment in capacity indicates the volume expansion during cycling as tin volume expands up to 300% during cycling and thus cause the electrolyte to wet new surfaces which ultimately yields capacity increment. On the other hand, the Sn-0.8V and Sn-0.9V cell, this volume expansion is not that vulnerable at the beginning of cycling. For Sn-0.8V cell, the capacity became stable after 3rd cycle and started decreasing after 8th cycle. While for Sn-0.9V cell, a small capacity increment was visible from 2nd to 3rd cycle which gradually increased to 800 mAh/g at 7th cycle. For both of them, the 1st lithiation capacities are 679 and 682 mAh/g as found in Figure 4B (green and red curve), respectively. Similar decline in capacity was found for this cell as well. Though all the four cells are indicating high initial Coulombic efficiency (CE) and a certain amount of volume expansion during cycling, this volume expansion is less intense for Sn-0.8V and Sn-0.9V cells, so these two cells were used for further electrochemical performance test and characterization. For further characterization, CV experiment was carried out for first two cycles and stated in Figure 4C and D. For the first cycle (Figure 4C), one lithium insertion peak appeared at 0.03V and 0.1V for Sn-0.8V and Sn-0.9V, respectively. The lithium extraction occurred in two steps, first one at 0.78 for Sn-0.8V; 0.73V for Sn-0.9V cell while the second peak appeared at 0.85V for both cells. For the second cycle, expressed with green color in Figure 4D, multiple lithiation and delithiation was observed. For Sn-0.8V cell, two weak peaks at 0.66 and 0.5V as well as two relatively intense peaks appeared at 0.32 and 0.2V. For Sn-0.9V CV, those weak peaks were visible almost at the same potential but this time only one lithium insertion occurred at 0.3V. First delithiation peaks shifted to the left at 0.72V and 0.68V for Sn-0.8V and Sn-0.9V, respectively. While the second peak appeared at the same potential as earlier for both CVs. For Sn-0.9V cell, a weak third delithiation peak was observed at 0.54V. To interpret these peaks, one must closely look at the Figure 4D. During the first lithiation where the potential is swept to towards positive voltages, the peak around -0.7V and -0.9V are related to the lithium alloying mechanism of tin particles following $4.4Li^+ + 4.4e^- + Sn \rightarrow Li_{4.4}Sn$ reaction order in multistep fashion. During the de-alloying the reversible dealloying mechanism follows the reaction mechanism of $Li_xSn \leftrightarrow Sn + xLi^+ + xe^-$ (Obrovac & Chevrier, 2014).

In order to increase and optimize the capacity as well as to improve the quality of the electrode, minimize the tin expansion and cracking during cycling, two different electrode engineering or modification were carried out namely, post deposition heat treatment and conductive polymer coating. Low temperature heat treatment was carried out in an oxygen free environment in order to prevent the oxidation of electrodeposited tin. For implementing this, tin was deposited on Cu foil at -0.8V and -0.9V as stated earlier and transferred into the glove box after properly drying it under dynamic vacuum prior to ethanol rinsing. Hot plate was used to heat up the single side tin deposited Cu foil at 100 0C for 30 min. Then coin cell was prepared as stated earlier. For conductive polymer coating, PVP was used after dissolving 5% (wt) in absolute ethanol. PVP ethanol solution was coated on the tin

deposited Cu foil (single side) by using the vacuum coating instrument at 200 rpm. After coating, the electrodes were dried under laboratory environment overnight to ensure complete drying of electrodes. Coin cell was prepared from these electrodes afterwards.

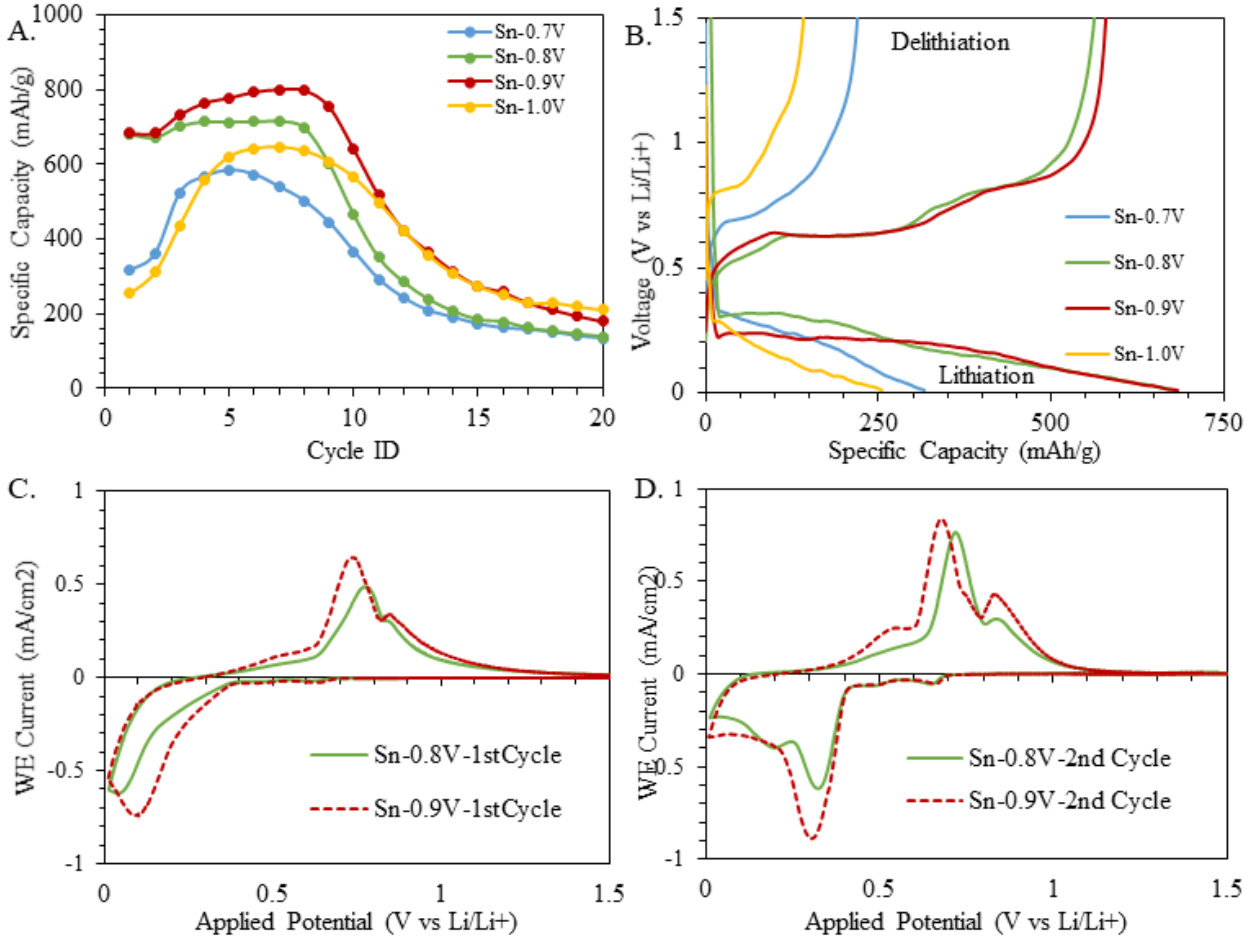

Figure 4. Electrochemical performance and characterization. A) Cycle life of electrodes made from four different constant voltage deposition, B) Charge-discharge profile for electrodes made from four different constant voltage deposition, C) 1st cycle CV for electrodes made from -0.8V and -0.9V constant voltage deposition and D) 2nd cycle CV for electrodes made from -0.8V and -0.9V constant voltage deposition.

The comparison results are expressed in Figure 5. The cells that were coated with PVP was named as Sn-0.8V-PVP, Sn-0.9V-PVP and cells prepared form heat treated electrodes were named as Sn-0.8V-HeatTreat and Sn-0.8V-HeatTreat. The charging capacity of these cells were compared with the untreated electrodes (dotted line in Figure 5). As we can observe from the Figure 5 that both heat treatment and polymer coating helped the electrodeposited tin electrodes to increase their first charging capacity 300 mAh/g more than untreated electrodes. PVP coating increased Sn-0.8V cell's capacity from 679 to 991 mAh/g (sky blue) while heat treatment at 100 0C increased it to 812 mAh/g (grey). For Sn-0.9V cell's, PVP coating increased the capacity to 922 (orange colored line) from 682 mAh/g and heat treatment increased it to 828 mAh/g (yellow colored line). The capacity decreased in second cycle and stabilized afterwards up until 6th cycles in both PVP coated and heat treated electrodes. This might be the indication of mitigation of tin expansion during cycling that happened in untreated electrodes (Sn-0.8V and Sn-0.96V). Increment in capacity occurs when anode expands and newer region get wetted by electrolyte which was not seen in PVP coated and heat treated electrodes might be suggesting the tin expansion was minimized or didn't occur. Among all the electrodes, PVP coated electrodes delivered the highest charging capacity might me due to the flexible polymer coating on the tin surface which is helping to keep connection between cracked region. Heat treatment also helping to

prevent expansion but at lower capacity might be due to the change in crystal structure or oxidation during heat treatment.

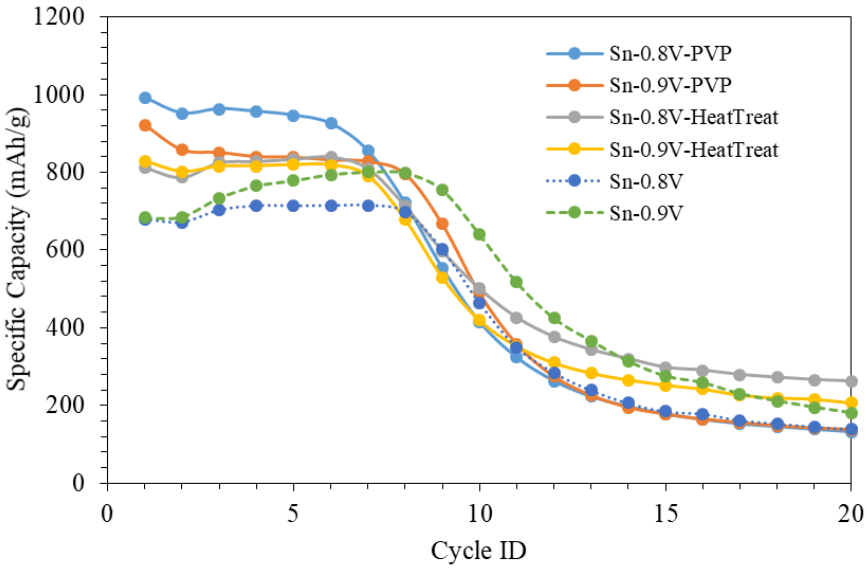

Figure 5. Charging capacity for polymer coated and heat treated electrodes

CONCLUSION

This study revealed that the particle morphology is highly dependent upon the deposition potential of tin in aqueous solution. Although XRD patterns did not reveal any significant difference, the particle growth mechanism is highly affected and the higher the deposition potential the larger the grain size of particles were observed from the SEM figures. Based on the electrochemical performances, among the studied deposition potentials, the mid-point, i.e. -0.9V, deposition found to be the optimum potential. The cycle life of the deposited samples at different potentials did not reveal any significant superiority among the samples, indicating inherent problems associated with the tin alloying mechanism. Neither heat treatment after the deposition nor the polymeric PVDC coating enhanced the cycle life properties of the deposited tin films.

ACKNOWLEDGEMENTS

MNA is thankful to Dr. Yusuf Öztürk and Dr. Özgür Duygulu for the XRD and SEM measurements, respectively. MNA is also indebted to TÜBİTAK for providing the grant of 2232-International Fellowship for Outstanding Researchers Programme (project no. 118C307).

Conflict of Interest

There is no conflict of interest.

REFERENCES

Abd El Rehim, S., Sayyah, S., & El Deeb, M. (2000). Electroplating of tin from acidic gluconate baths. *PLATING & SURFACE FINISHING*.

Ashworth, M. A., Wilcox, G. D., Higginson, R. L., Heath, R. J., Liu, C., & Mortimer, R. J. (2015). The effect of electroplating parameters and substrate material on tin whisker formation. *Microelectronics Reliability*, *55*(1), 180-191. doi:https://doi.org/10.1016/j.microrel.2014.10.005

Ates, M. N., & Busbee, J. (2017). Electrodeposition of Metal Oxide Nanoparticles for Li-Ion Battery Anodes. *ECS Meeting Abstracts, MA2017-02*(4), 415. doi:10.1149/MA2017-02/4/415

Derrien, G., Hassoun, J., Panero, S., & Scrosati, B. (2007). Nanostructured Sn–C Composite as an Advanced Anode Material in High-Performance Lithium-Ion Batteries. *19*(17), 2336-2340. doi:https://doi.org/10.1002/adma.200700748

Dirican, M., Yanilmaz, M., Fu, K., Lu, Y., Kizil, H., & Zhang, X. (2014). Carbon-enhanced electrodeposited SnO2/carbon nanofiber composites as anode for lithium-ion batteries. *Journal of Power Sources, 264*, 240-247. doi:https://doi.org/10.1016/j.jpowsour.2014.04.102

Han, C., Liu, Q., & Ivey, D. G. (2009). Nucleation of Sn and Sn–Cu alloys on Pt during electrodeposition from Sn–citrate and Sn–Cu–citrate solutions. *Electrochimica Acta, 54*(12), 3419-3427. doi:https://doi.org/10.1016/j.electacta.2008.12.064

He, A., Liu, Q., & Ivey, D. G. (2008). Electrodeposition of tin: a simple approach. *Journal of Materials Science: Materials in Electronics, 19*(6), 553-562. doi:10.1007/s10854-007-9385-3

Huang, X., Chen, Y., Fu, T., Zhang, Z., & Zhang, J. (2013). Study of Tin Electroplating Process Using Electrochemical Impedance and Noise Techniques. *Journal of the Electrochemical Society, 160*(11), D530. doi:10.1149/2.055311jes

Kong, Z., Zhang, K., Huang, M., Tu, H., Yao, X., Shao, Y., Hao, X. (2022). Stabilizing Sn anodes nanostructure: Structure optimization and interfacial engineering to boost lithium storage. *Electrochimica Acta, 405*, 139789. doi:https://doi.org/10.1016/j.electacta.2021.139789

Lee, J.-Y., Kim, J.-W., Chang, B.-Y., Tae Kim, H., & Park, S.-M. (2004). Effects of Ethoxylated α-Naphtholsulfonic Acid on Tin Electroplating at Iron Electrodes. *Journal of the Electrochemical Society, 151*(5), C333. doi:10.1149/1.1690289

Mao, O., Dunlap, R. A., & Dahn, J. R. (1999). Mechanically Alloyed Sn-Fe(-C) Powders as Anode Materials for Li-Ion Batteries: I. The Sn2Fe - C System. *Journal of the Electrochemical Society, 146*(2), 405. doi:10.1149/1.1391622

Obrovac, M. N., & Chevrier, V. L. (2014). Alloy Negative Electrodes for Li-Ion Batteries. *Chemical Reviews, 114*(23), 11444-11502. doi:10.1021/cr500207g

Sohel, I. H., Öztürk, T., Aydemir, U., Peighambardoust, N. S., Duygulu, Ö., Işık-Gülsaç, I., Ateş, M. N. (2022). Deciphering the effect of the heat treatment on the electrodeposited silicon anode for Li-ion batteries. *Journal of Energy Storage, 55*, 105817. doi:https://doi.org/10.1016/j.est.2022.105817

Tirado, J. L. (2003). Inorganic materials for the negative electrode of lithium-ion batteries: state-of-the-art and future prospects. *Materials Science and Engineering: R: Reports, 40*(3), 103-136. doi:https://doi.org/10.1016/S0927-796X(02)00125-0

Torrent-Burgués, J., Guaus, E., & Sanz, F. (2002). Initial stages of tin electrodeposition from sulfate baths in the presence of gluconate. *Journal of Applied Electrochemistry, 32*(2), 225-230. doi:10.1023/A:1014710500122

Ui, K., Kikuchi, S., Kadoma, Y., Kumagai, N., & Ito, S. (2009). Electrochemical characteristics of Sn film prepared by pulse electrodeposition method as negative electrode for lithium secondary batteries. *Journal of Power Sources, 189*(1), 224-229. doi:https://doi.org/10.1016/j.jpowsour.2008.09.081

Walsh, F. C., & Low, C. T. J. (2016). A review of developments in the electrodeposition of tin. *Surface and Coatings Technology, 288*, 79-94. doi:https://doi.org/10.1016/j.surfcoat.2015.12.081

Wang, B., Luo, B., Li, X., & Zhi, L. (2012). The dimensionality of Sn anodes in Li-ion batteries. *Materials Today, 15*(12), 544-552. doi:https://doi.org/10.1016/S1369-7021(13)70012-9

Wu, M., Wang, C., Chen, J., Wang, F., & Yi, B. (2013). Sn/carbon nanotube composite anode with improved cycle performance for lithium-ion battery. *Ionics, 19*(10), 1341-1347. doi:10.1007/s11581-013-0870-9

Yue, X., Johnson, A. C., Kim, S., Kohlmeyer, R. R., Patra, A., Grzyb, J., Pikul, J. H. (2021). A Nearly Packaging-Free Design Paradigm for Light, Powerful, and Energy-Dense Primary Microbatteries. *33*(35), 2101760. doi:https://doi.org/10.1002/adma.202101760

Zhang, Y., & Abys, J. A. (1999). A unique electroplating tin chemistry. *Circuit World, 25*(1), 30-37. doi:10.1108/03056129910244815

Zheng, Z., Chen, B., Xu, Y., Fritz, N., Gurumukhi, Y., Cook, J., Wang, P. (2020). A Gaussian Process-Based Crack Pattern Modeling Approach for Battery Anode Materials Design. *Journal of Electrochemical Energy Conversion and Storage, 18*(1). doi:10.1115/1.4046938